

Current Biology

Insights into the Evolution of Multicellularity from the Sea Lettuce Genome

Highlights

- The *Ulva* genome is the first whole-genome sequence of a green seaweed
- Gene families associated with multicellularity are distinct from freshwater algae
- Cell-cycle S-phase entry does not depend on the RB/E2F pathway or D-type cyclins
- *Ulva*, a renowned DMS-producer, uses homologs of the Alma protein to cleave DMSP

Authors

Olivier De Clerck, Shu-Min Kao, Kenny A. Bogaert, ..., Yves Van de Peer, Thomas Wichard, John H. Bothwell

Correspondence

olivier.declerck@ugent.be (O.D.C.),
j.h.bothwell@durham.ac.uk (J.H.B.)

In Brief

De Clerck et al. present the first genome sequence of a green seaweed, a dominant group of primary producers in coastal environments. The *Ulva* genome informs on an independent acquisition of multicellularity, sheds light on adaptations to life in intertidal habitats, and identifies candidate genes involved in DMSP biosynthesis and conversion to DMS.

Insights into the Evolution of Multicellularity from the Sea Lettuce Genome

Olivier De Clerck,^{1,21,*} Shu-Min Kao,^{2,3} Kenny A. Bogaert,¹ Jonas Blomme,^{1,2} Fatima Foflonker,⁴ Michiel Kwantes,⁵ Emmelien Vancaester,^{2,3} Lisa Vanderstraeten,⁶ Eylem Aydogdu,^{2,3} Jens Boesger,⁵ Gianmaria Califano,⁵ Benedicte Charrier,⁷ Rachel Clewes,⁸ Andrea Del Cortona,^{1,2,3} Sofie D'Hondt,¹ Noe Fernandez-Pozo,⁹ Claire M. Gachon,¹⁰ Marc Hanikenne,¹¹ Linda Lattermann,⁵ Frederik Leliaert,^{1,12} Xiaojie Liu,¹ Christine A. Maggs,¹³ Zoë A. Popper,¹⁴ John A. Raven,^{15,16} Michiel Van Bel,^{2,3} Per K.I. Wilhelmsson,⁹ Debashish Bhattacharya,⁴ Juliet C. Coates,⁸ Stefan A. Rensing,⁹ Dominique Van Der Straeten,⁶ Assaf Vardi,¹⁷ Lieven Sterck,^{2,3} Klaas Vandepoele,^{2,3,19} Yves Van de Peer,^{2,3,18,19} Thomas Wichard,⁵ and John H. Bothwell^{20,*}

¹Biology Department, Ghent University, 9000 Ghent, Belgium

²Department of Plant Biotechnology and Bioinformatics, Ghent University, Technologiepark 927, 9052 Ghent, Belgium

³VIB Center for Plant Systems Biology, Technologiepark 927, 9052 Ghent, Belgium

⁴Department of Biochemistry and Microbiology, Rutgers University, New Brunswick, NJ 08901, USA

⁵Institute for Inorganic and Analytical Chemistry, Jena School for Microbial Communication, Friedrich Schiller University Jena, Lessingstr. 8, 07743 Jena, Germany

⁶Laboratory of Functional Plant Biology, Department of Biology, Ghent University, K.L. Ledeganckstr. 35, 9000 Ghent, Belgium

⁷Morphogenesis of Macroalgae, UMR8227, CNRS-UPMC, Station Biologique, Roscoff 29680, France

⁸School of Biosciences, University of Birmingham, Edgbaston, B15 2TT, UK

⁹Faculty of Biology, University of Marburg, Karl-von-Frisch-Str. 8, 35043 Marburg, Germany

¹⁰Scottish Association for Marine Science, Scottish Marine Institute, Oban, PA37 1QA, UK

¹¹InBioS-Phytosystems, University of Liège, 4000 Liège, Belgium

¹²Botanic Garden Meise, Nieuwelaan 38, 1860 Meise, Belgium

¹³School of Biological Sciences and Queen's University Marine Laboratory Portaferry, Queen's University Belfast, Northern Ireland, BT7 1NN, UK

¹⁴Botany and Plant Science and Ryan Institute for Environmental, Marine, and Energy Research, School of Natural Sciences, National University of Ireland, Galway, Galway, Ireland

¹⁵Division of Plant Sciences, University of Dundee at the James Hutton Institute, Dundee, DD2 5DA, UK

¹⁶School of Biological Sciences, University of Western Australia (M048), 35 Stirling Highway, WA 6009, Australia

¹⁷Department of Plant and Environmental Sciences, Weizmann Institute of Science, 76100 Rehovot, Israel

¹⁸Department of Genetics, Genomics Research Institute, University of Pretoria, Pretoria 0028, South Africa

¹⁹Bioinformatics Institute Ghent, Ghent University, Technologiepark 927, 9052 Ghent, Belgium

²⁰School of Biological and Biomedical Sciences and Durham Energy Institute, Durham University, Durham, DH1 3LE, UK

²¹Lead Contact

*Correspondence: olivier.declerck@ugent.be (O.D.C.), j.h.bothwell@durham.ac.uk (J.H.B.)

<https://doi.org/10.1016/j.cub.2018.08.015>

SUMMARY

We report here the 98.5 Mbp haploid genome (12,924 protein coding genes) of *Ulva mutabilis*, a ubiquitous and iconic representative of the Ulvophyceae or green seaweeds. *Ulva*'s rapid and abundant growth makes it a key contributor to coastal biogeochemical cycles; its role in marine sulfur cycles is particularly important because it produces high levels of dimethylsulfoniopropionate (DMSP), the main precursor of volatile dimethyl sulfide (DMS). Rapid growth makes *Ulva* attractive biomass feedstock but also increasingly a driver of nuisance "green tides." Ulvophytes are key to understanding the evolution of multicellularity in the green lineage, and *Ulva* morphogenesis is dependent on bacterial signals, making it an important species with which to study cross-kingdom communication. Our sequenced genome informs these aspects of ulvophyte cell biology, physiology, and ecology. Gene family ex-

pansions associated with multicellularity are distinct from those of freshwater algae. Candidate genes, including some that arose following horizontal gene transfer from chromalveolates, are present for the transport and metabolism of DMSP. The *Ulva* genome offers, therefore, new opportunities to understand coastal and marine ecosystems and the fundamental evolution of the green lineage.

INTRODUCTION

Transitions from microscopic, unicellular life forms to complex multicellular organisms are relatively rare events but have occurred in all major eukaryotic lineages, including animals, fungi, and plants [1, 2]. Algae, having acquired complex multicellularity several times independently, provide unique insights into the underlying mechanisms that facilitate such transitions. In the green lineage, there have been several independent transitions to multicellularity. Within Streptophyta, the origin of complex land plants from a green algal ancestor was preceded by a series

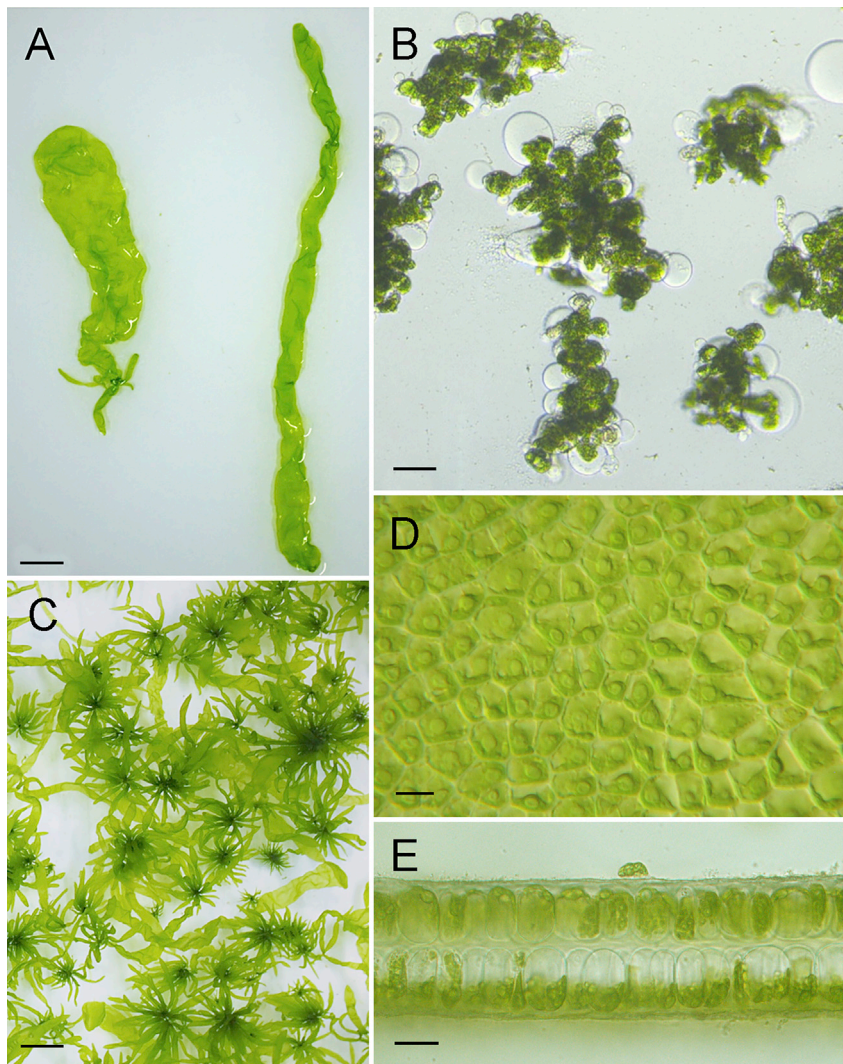


Figure 1. Morphology and Anatomy of *Ulva mutabilis*

(A) External morphology of a blade (left) and tubular thallus (right). Both growth forms are part of the naturally occurring morphological variation (bar: 1 cm).

(B) Axenically developing *Ulva* with a typical callus-like morphology without cell differentiation. Protrusions of the malformed exterior cell wall are visible (bar: 100 μ m).

(C) Batch culture under standardized conditions associated with two bacterial strains, *Roseovarius* sp. MS2 and *Maribacter* sp. MS6 (bar: 1 cm).

(D) Surface of a blade with cells containing a single chloroplast and pyrenoid (differential interference contrast; bar: 15 μ m).

(E) Transverse section of a typical *Ulva*-type blade with two cell layers (*U. rigida*; bar = 20 μ m).

cells thick or as tubes one-cell thick (Figure 1A). Both forms co-occur in most clades, as well as within single species. These morphologies, however, are only established in the presence of appropriate bacterial communities [11]. In axenic culture conditions, *Ulva* grows as a loose aggregate of cells with malformed cell walls (Figure 1B). Only when it is exposed to certain bacterial strains (e.g., *Roseovarius* and *Maribacter*) or grown in conditioned medium is complete morphogenesis observed [11]. Thallusin, a chemical cue inducing morphogenesis, has been characterized for the related genus *Monostroma* [12], and additional substances that induce cell division (*Roseovarius* factor) and cell differentiation (*Maribacter* factor) have been partially purified

of morphological, cytological, and physiological innovations that began long before the colonization of land [3]. Within the Chlorophyta, the transition from uni- to multicellularity has occurred in several clades and has been studied particularly extensively in the volvocine lineage [4]. Comparative genomic analyses between unicellular (*Chlamydomonas*), colonial (*Gonium*, *Tetra-baena*), and multicellular (*Volvox*) species revealed protein-coding regions to be very similar, with the notable exceptions of the expansion of gene families involved in extracellular matrix (ECM) formation and cell-cycle regulation [5–7].

The Ulvophyceae, or green seaweeds, represent an independent acquisition of a macroscopic plant-like vegetative body known as a thallus. Ulvophyceae display an astounding morphological and cytological diversity [8] that includes unicells, filaments, and sheet-like thalli, as well as giant-celled coenocytic or siphonous seaweeds [9]. *Ulva*, or sea lettuce, is by far the best-known representative of the Ulvophyceae and is well established as a model organism for studying morphogenesis in green seaweeds [10]. The *Ulva* thallus is relatively simple, with small uninucleate cells and a limited number of cell types. *Ulva* exists in the wild in two forms: either as flattened blades that are two-

from *Ulva*-associated bacteria [11]. The value of *Ulva* as a model organism for green seaweed morphogenesis is enhanced by its tractability for genetic analyses. Under laboratory conditions, individuals readily complete the life cycle, which involves an alternation of morphologically identical haploid gametophytes and diploid sporophytes [10]. Furthermore, a stable polyethylene glycol (PEG)-based genetic transformation system is available [13].

The *Ulva* genus is also of great ecological significance. *Ulva* is widely distributed along tropical and temperate coasts, and several species penetrate freshwater streams and lakes. Under high-nutrient conditions, *Ulva* can give rise to spectacular blooms known as “green tides,” often covering several hundreds of kilometers of coastal waters. Beached algae may amount to a million tons of biomass and smother entire coastlines and negatively impact tourism and local economies [14]. Although not toxic, green tides have led to fatalities due to the hydrogen sulphide that is formed when the dead biomass decays. Despite the harmful consequences of *Ulva*’s rapid growth rate, beneficial aspects include exploitation of its biomass—e.g., for biofuel production, protein for animal feed, and the removal of excess nutrients in integrated multitrophic aquaculture systems [15].

<i>Ulva mutabilis</i> : summary statistics	
Genome size (Mbp)	98.5
Scaffold N50 (Mbp)	0.6
Percentage GC	57.2
Number of protein coding genes	12,924
Gene density (genes/Mb)	131.2
Average intron per gene	3.9
Average exon length (bp)	303.1
Average intron length (bp)	368.6
Percentage of genes with introns	85.0

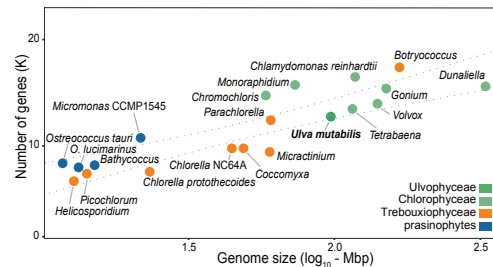


Figure 2. Summary Statistics for the *Ulva mutabilis* Genome

Comparison of genome size and number of protein-coding genes among green algal genomes. Color coding indicates classes.

See also Figure S2, Table S1, and Table S2.

The genomic resources for the Ulvophyceae that could shed light on their independent transition to multicellularity and the evolution of the cyto-morphological diversity are limited to a transcriptomic study of *U. linza* [16] and a description of the mating-type locus of *U. partita* [17]. In addition, Ranjan and colleagues [18] studied the distribution of transcripts in the thallus of the siphonal green seaweed *Caulerpa*. Here, we present the first whole-genome sequence of an *Ulva* species, *U. mutabilis* Føyn (Figure 1). The species is phylogenetically closely related to *U. compressa* Linnaeus (Figure S1), a widespread species known to form nuisance blooms. The sequenced strain was isolated from southern Portugal [19] and has been successfully maintained in culture. Several important aspects of its biology, including cell cycle, cytology, life-cycle transition, induction of spore and gamete formation, and bacterial-controlled morphogenesis, have been studied in detail over the past 60 years [10]. We intend our *Ulva* genome, in combination with the availability of a genetic toolkit and developmental and life-cycle mutants, to spur the new developmental research in green seaweeds that will be critical if we are to harness their aquaculture potential while mitigating the threat from blooms. Our analyses of the *Ulva* genome reveal features that underpin the development of a multicellular thallus and expansion of gene families linked to the perception of photoperiodic signals and abiotic stress, which are key factors for survival in intertidal habitats. Furthermore, we unveil key genes involved in the biosynthesis of dimethylsulfoniopropionate (DMSP) and dimethyl sulfide (DMS), important signaling molecules with a critical role in the global sulfur cycle.

RESULTS AND DISCUSSION

Genome Sequencing and Gene-Family Evolution

The genome size of *U. mutabilis* was estimated by flow cytometry and k-mer spectral analysis to be around 100 Mbp. In total, 6.9 Gbp of PacBio long reads were assembled into 318 scaffolds (98.5 Mbp), covering 98.5% of the estimated nuclear haploid genome (Figure 2 and Table S1). To increase the accuracy of the genome sequence at single-base resolution, the scaffolds were polished using PacBio and Illumina paired-end reads. We predicted 12,924 protein-coding genes, of which 91.8% were supported by RNA sequencing (RNA-seq) data. Analyses of genome completeness indicated that the genome assembly captures at least 92% of the eukaryotic BUSCO dataset. Analyses of pico-PLAZA core gene families resulted in a completeness score of 0.968 of the protein-coding genes (Table S2). Annotation of repetitive elements resulted in 35% of the genome being masked. Among the identified repeats, 74% were classi-

fied as known or reported repeat families, with long terminal repeats (LTRs) and long interspersed elements (LINES) being predominant, representing 15.3 Mbp and 9.3 Mbp, respectively (Table S3).

The *Ulva* genome size is intermediate between sequenced genomes in the Chlorophyceae and Trebouxiophyceae (Figure 2). The number of predicted genes and gene families is markedly lower compared to most Chlorophyceae, including the volvocine algae (*Chlamydomonas*, *Gonium*, *Tetraabaena*, and *Volvox*), but higher than the Trebouxiophyceae and prasinophytes (Figures 2 and 3). The relative gene family sizes, however, are roughly equal between *Ulva* and volvocine algae when corrected for total genome size (Figure S2). A phylogenetic tree inferred from a concatenated alignment of 58 nuclear protein-coding genes (totaling 42,401 amino acids) supports a sister-group relationship of *Ulva* with the Chlorophyceae in the crown chlorophytes (Figure 3). This topology corroborates earlier phylogenetic hypotheses based on multigene organelle datasets (reviewed in [8]). The divergence of *Ulva* and the *Chlamydomonas-Gonium-Volvox* clade (Chlorophyceae, Volvocales) from their common ancestor coincided with substantial gain and loss of gene families in both lineages (Figure 3). Gain and loss, however, do not seem to be correlated with multicellularity.

Evolution of Multicellularity

Ulva develops from gametes or zoospores into a multicellular thallus consisting of three main cell types (rhizoid, stem, and blade cells). After a first division, the basal cell gives rise to a rhizoidal cell and the apical cell [20]. Subsequent morphogenesis is then governed by a progressive change in cell cycles. The growth rate of the basal cells decreases after a few cell cycles, so that the holdfast remains small, while the division of blade cells continues and becomes synchronized to the prevailing light:dark cycle [20]. The shape of the multicellular thallus in *Ulva* is therefore largely driven by how cell size and division are controlled, and many morphological mutants in *U. mutabilis*, including the slender mutant used in this study (see below), appear to have arisen from underlying changes in cell-cycle regulation [20].

The evolution of a complex thallus morphology is often associated with expansions in gene families that are involved in cell signaling, transcriptional regulation, and cell adhesion [1]. The *Ulva* genome encodes 251 proteins involved in transcriptional regulation—a comparatively low number for a green alga—which is also reflected in a low fraction of such proteins encoded by the genome (1.94% when compared to the average of 2.66% in green algae). *Ulva* lacks 10 families of transcription factors (TFs) and two families of transcriptional regulators (TRs) that are present in other green algae

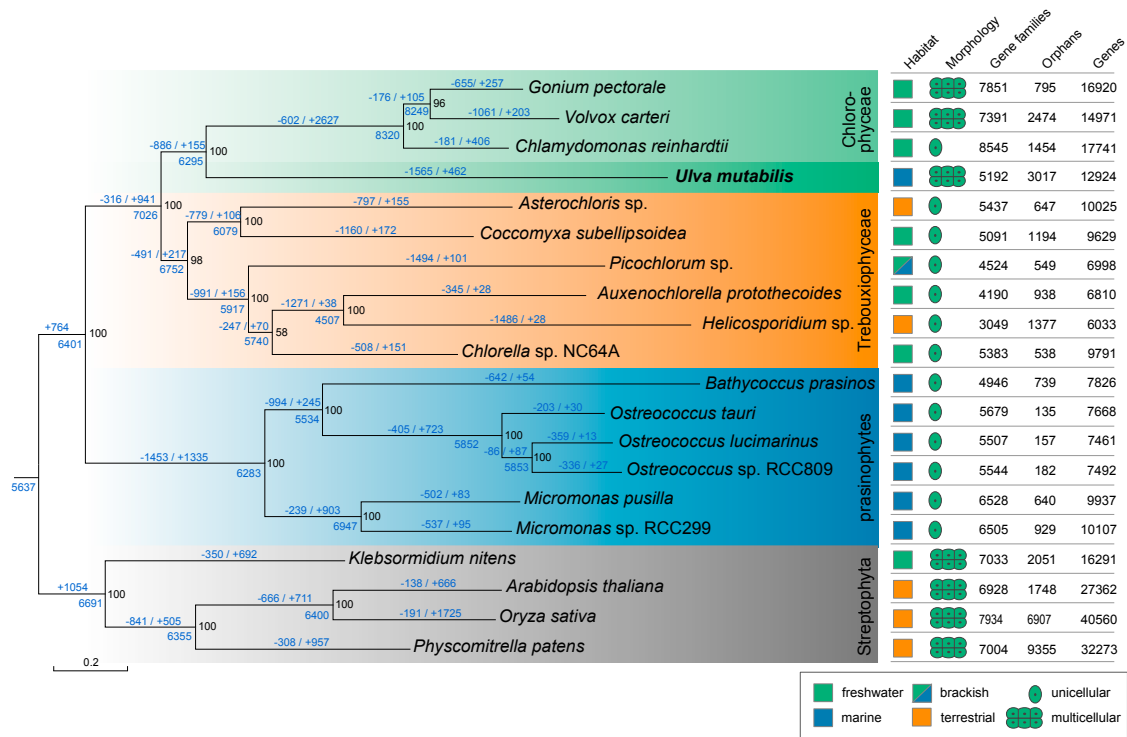


Figure 3. Predicted Pattern of Gain and Loss of Gene Families during the Evolution of Green Algae and Land Plants

For each species, the total number of gene families, the number of orphans (genes that lack homologues in the eukaryotic data set), and the number of genes are indicated, as well as habitat and morphological characteristics. Maximum likelihood bootstrap values are indicated in black at each node. The number of gene families acquired or lost (values indicated in blue along each branch in the tree) was estimated using the Dollo parsimony principle.

(Data S1). Furthermore, the existing transcription-associated protein families are, on average, smaller than those in other green algae (Figure 4A).

Among the most remarkable gene families that have been lost are genes of the retinoblastoma (RB)/E2F pathway and associated D-type cyclins. Comparative genomic studies of volvocine algae have revealed that the co-option of the RB cell-cycle pathway is a key step towards multicellularity in this group of green algae [5–7]. Apart from implying that evolution toward multicellularity progressed along different trajectories in *Ulva* and the volvocine algae, the absence of D-type cyclins, RB, and E2F signifies that entry into the cell cycle and the G1-S transition are independent on these genes, as is the case in yeast. As no homologs of Cln 2/3, SBF, and Whi5, which mediate G1-S transition in yeast [22], are found in *Ulva*, we hypothesize that either a functionally analogous set of genes or an entirely different mechanism regulates *Ulva* S-phase entry. Interestingly, RB and E2F homologs were found in the transcriptome of the siphonous ulvophyte *Caulerpa* [18], so at present, it remains unclear how widely the RB/E2F pathway is conserved within the Ulvophyceae. Other aspects of the cell cycle are more in line with other green algae (Figure S4 and Data S1), be it that the single CDKA homolog (UM001_0289) contains a modified cyclin-binding motif, PSTALRE, instead of the evolutionarily conserved PSTAIRE motif. While variations in this motif are not uncommon in eukaryotes, *Ulva* is the first member of the green lineage to have such a variation reported.

Contrary to the expectation for a multicellular organism [23], few TF families are expanded in *Ulva* (Figure 4A). Notable exceptions are CONSTANS-LIKE (CO-like) TFs, of which *Ulva* has five genes, whereas all other sequenced algae encode between zero and two (Figures 4A and 4B). These CO-like TFs are characterized by one or two (group II or III) zinc-finger B boxes and a CCT protein domain. Both protein domains are involved in protein-protein interactions, and the CCT domain mediates DNA binding in a complex with HEME ACTIVATOR PROTEIN (HAP)-type TFs in *Arabidopsis* [21]. *Ulva* CO-like proteins form a single clade within other algal lineages (Figure 4B). In addition to the five CO-like TFs, functionally related proteins containing either (1) only a B-box domain similar to group V B-Box zinc fingers [21] or (2) only a CCT domain and belonging to the CCT motif family [24] are also expanded in *Ulva*. B-box zinc fingers and CMF proteins in angiosperms have been implicated in developmental processes such as photoperiodic flowering [25], regulation of circadian rhythms [26], and abiotic stress responses [27]. The control of light and photoperiod signaling is conserved in the green algae *C. reinhardtii* and *Ostreococcus tauri* [28, 29]. Moreover, the CO-like TFs are one of the families potentially involved in the establishment of complex multicellularity in green algae and land plants [30]. Genome-wide mapping of *Ulva* CO-like genes and functionally related genes indicates that the majority (60%) originated through tandem duplication in *Ulva* (Figure 4C). Although the functions of these proteins will need to be confirmed experimentally, the CO-like and CMF genes in *Ulva*

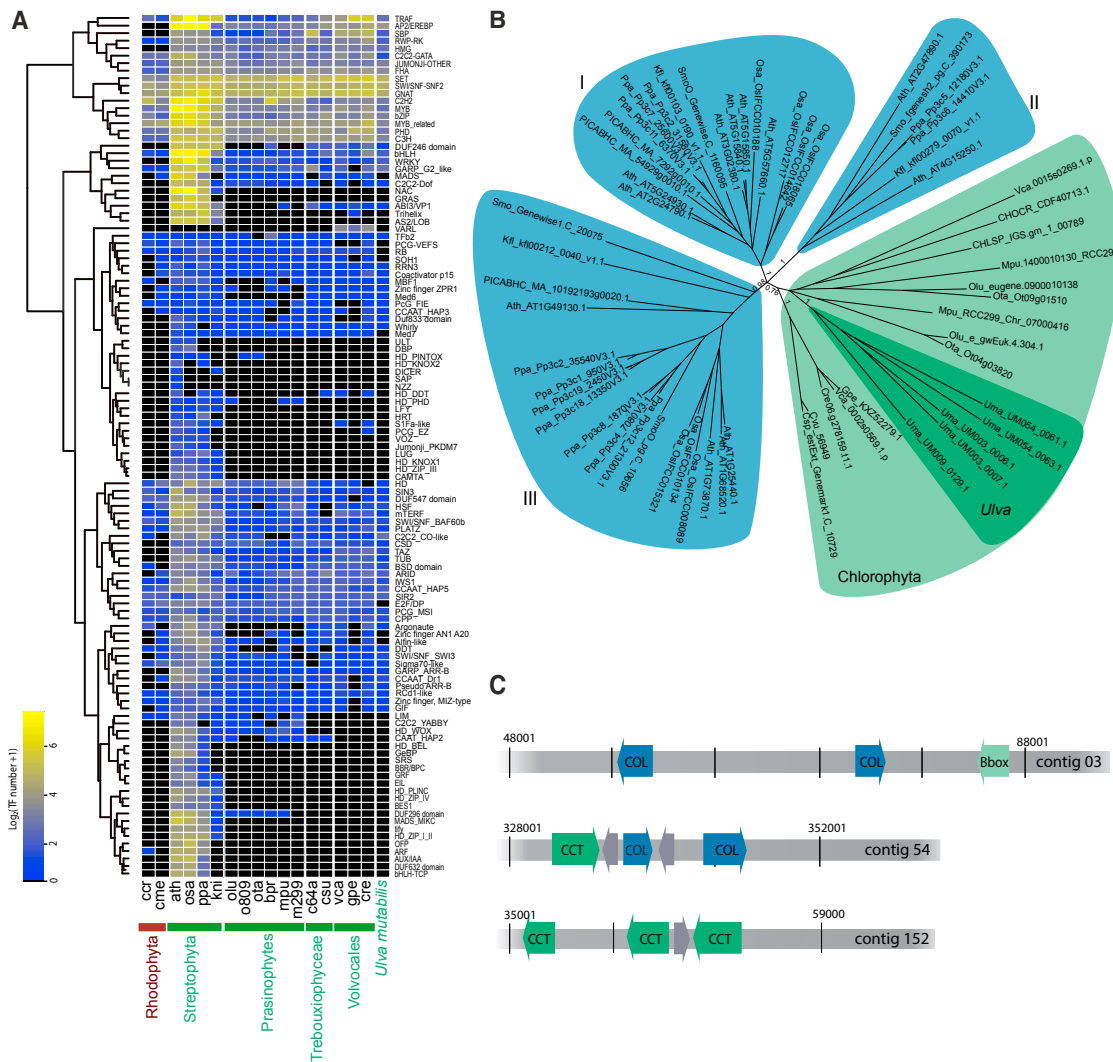


Figure 4. Comparative Analysis of Transcription-Associated Proteins

(A) Heatmap of transcription factors comparing *Ulva* with a selection of green algae (*Bathycoccus prasinos*, bpr; *Chlamydomonas reinhardtii*, cre; *Chlorella variabilis*, CN64a; *Gonium pectorale*, gpe; *Micromonas pusilla*, mpu; *Micromonas* sp., m299; *Ostreococcus lucimarinus*, olu; *O. tauri*, ota and o809; *Coccomyxa subellipsoidea*, cvu; *Volvox carterii*, vca), streptophytes (*Klebsormidium nitens*, kni), land plants (*Arabidopsis thaliana*, ath; *Oryza sativa*, osa; *Physcomitrella patens*, ppa), and red algae (*Chondrus crispus*, ccr; *Cyanidioschyzon merolae*, cme).

(B) Maximum likelihood phylogeny of CO-like transcription factors that are expanded in *Ulva*. Roman numbers refer to the classification as in Khanna et al. [21].

(C) Examples of tandem distributions of *Ulva* CO-like genes (containing a CCT and B-box domain) and genes containing either a CCT or B-box domain on contigs 003, 053, and 154.

See also [Data S1](#).

could be involved in the integration of a multitude of environmental signals in a highly dynamic intertidal environment—a kind that the other sequenced green algae are not regularly subjected.

A total of 441 protein kinases were identified in the *Ulva* genome, representing about 3%–4% of all protein-coding genes. The largest subfamily of *Ulva* kinases has similarity to PKnB kinase (Data S1), a “eukaryotic-like” serine/threonine kinase originally discovered in bacteria. Around 20 of the PKnB kinases possess a transmembrane (TM) domain and an extracellular/adhesion domain—either Kringle (IPR000001), FAS1 (fasciclin-like; IPR000782), or Pectin lyase fold (IPR012334,

IPR011050)—and so represent good candidates for *Ulva* receptor kinases, with potential roles in environmental sensing and/or developmental signaling. By acting on *Ulva* cell wall components, for example, the pectin-lyase-fold domains may contribute to desiccation resistance [31] and to the growth and development of a multicellular thallus [32]. We note that although the three aforementioned extracellular domains are present in many green algae, including the green seaweed *Caulerpa* (Figure 5), it is unusual to see them linked to a kinase, and this coupling is only seen in a few other eukaryotic species. The Kringle-kinase domain combination, for instance, was initially discovered in animal receptor tyrosine kinase-like orphan

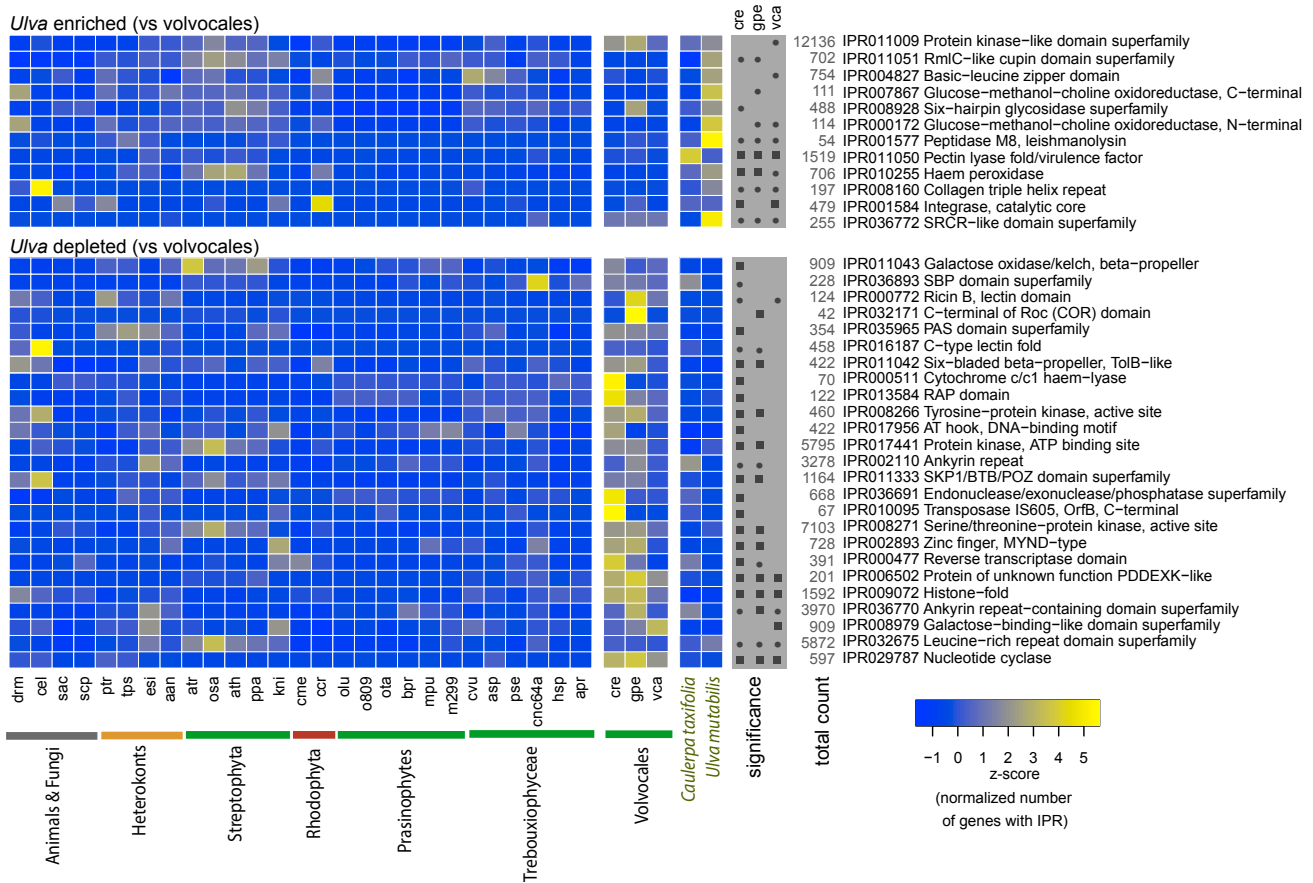


Figure 5. Comparative Analysis of Enriched and Depleted InterPro Domains in *Ulva mutabilis*

Significant differences relative to *Chlamydomonas reinhardtii*, *Volvox carteri*, and/or *Gonium pectorale* (Fisher's exact test, false discovery rate [FDR]-corrected $p < 0.05$) are denoted with squares if significant in *Ulva* and *Caulerpa* and circles if significant in *Ulva* only. Z scores represent the number of IPR hits normalized by the total number of hits per species.

See Table S7 for abbreviations used.

receptors (RORs), which use Wnt signaling proteins as ligands and function in multicellular development, neuronal outgrowth, cell migration, and polarity [33]. Our analysis additionally finds this domain combination in *Ulva* and the unicellular prasinophyte green algae (*Ostreococcus*). The Fasciclin-kinase combination is unique to *Ulva*, while the pectin-lyase-kinase combination is found only in the multicellular algae *Ulva*, *Klebsormidium*, and *Ectocarpus*. It is possible that *Ulva* Kringle-TM-kinase gene families arose via divergent evolution from a common ancestor based on sequence similarity of family members and the close proximity of some family members on single DNA scaffolds. The pectin-lyase-TM-kinase family proteins, on the other hand, are more divergent in sequence and structure (including kinase-TM-pectin-lyase proteins) and are more likely to have arisen by dynamic gene fusions or conversions.

In addition to containing extracellular protein domains that are linked to intracellular kinases, *Ulva* also shows a significantly enriched diversity of the protein domains associated with the ECM and cell surface relative to its sequenced sister taxa. Notable examples of these enriched ECM-associated domains include scavenger receptor cysteine-rich (SRCR) domain proteins (IPR001190, IPR017448), which are absent from land plants

but present in animals and Volvocales [34]. In Metazoans, the SRCR proteins have diverse roles that include the recognition of the pathogen-associated molecular patterns (PAMPs) that mediate bacterial interactions [35] and possibly encompass an early evolutionary role in cell-cell recognition or aggregation [36]. The germin (IPR001929) and RmlC-like cupin (IPR011051) domain folds are also among the ECM-associated domains and occur ubiquitously in streptophytes, where they are linked to the regulation of cell-wall properties such as extensibility and defense [37].

The gametolysin/MEROPS peptidase family M11 of *Volvox* matrix metalloproteases (VMPs) (IPR008752)—similar to mammalian collagenases and crucial to ECM remodeling [38]—is enriched in *Volvox* relative to *Chlamydomonas* [6]. While this M11 class of peptidases is itself absent in *Ulva*, the related MEROPS M8/leishmanolysin peptidase domain (IPR001577) is 23-fold enriched compared to *Chlamydomonas*. Additionally, 28 collagen triple helix repeat (IPR008160) proteins, with predicted extracellular locations, have been detected, each with a G-N/D-E repeat rather than the more usual G-P-Hyp, which suggests the presence of collagen-like innovations in the ECM of *Ulva*.

Phytohormones

The processes of growth and development in land plants are modulated by plant hormones, and experimental studies have suggested that such hormones may also be involved in *Ulva* morphogenesis to give a blade- or tube-like thallus [39]. However, because bacteria can produce plant hormones, it has not been clarified whether hormones previously detected in *Ulva* arose from the alga or from its associated bacteria. To add to the confusion, the *Roseovarius*-factor resembles a cytokinin, and the *Maribacter*-factor acts in a similar fashion to auxin, so bacteria-derived compounds may contribute to the development of the multicellular *Ulva* thallus [11]. We therefore investigated whether biosynthesis pathways for known phytohormones are present in *Ulva* and/or the associated bacteria and tested whether phytohormones could replace the bacterial morphogenetic factors. Homologs of plant hormone biosynthesis genes provided circumstantial evidence for the biosynthesis of abscisic acid (ABA), ethylene (ET), and salicylic acid (SA) in *Ulva* (Figure 6 and Data S1). Corroborating these results, we found that both xenic and axenic *Ulva* produce not just ABA, ET, and SA, but also auxin (IAA) and gibberellin (GA₃) (Table S4). Measurements of IAA in axenic cultures are more difficult to reconcile with the *Ulva* gene content, as little or no evidence was found for indole-3-pyruvic acid (IPA), tryptamine (TAM), and indole-3-acetamide (IAM) pathways. In *Ulva*, therefore, biosynthesis of IAA seems most likely to involve a pathway through indole-3-acetaldoxime and indole-3-acetaldehyde catalyzed by the AMI1 and AAO1 genes, respectively, that are found in the *Ulva* genome. The presence of GA₃ remains equivocal. In line with earlier findings [40], traces of GA₃ could be detected in both axenic and xenic slender cultures, but not in wild-type. At present, it is also unclear how to reconcile these traces of GA₃ with the gene content of *Ulva*, since the enzymes known to mediate the biosynthesis of the GA₃ precursor, *ent*-kaurene, in the plastid (CPP synthase, *ent*-kaurene synthase) are missing from the genome. We also found that the associated bacteria *Roseovarius* sp. MS2 and *Maribacter* sp. MS6 are able to produce IAA, GA₃, ET, SA, and the cytokinins (isopentenyladenine, iP) (Table S4). Despite this strong evidence for the synthesis of known phytohormones by *Ulva* and its associated bacteria, we observed that none of the tested hormones were able to trigger growth or development of gametes and young propagules in standardized bioassays (Figure S3). While the *Ulva* genome contained candidate genes for phytohormone biosynthesis, the corresponding angiosperm receptors were absent, corroborating the comparative genomic analyses by Wang et al. [41]. These authors found little evidence for the emergence of homologous plant hormone signaling pathways outside the charophyte lineage. Our findings, however, do not preclude hormonal or other functions for these products, using different pathways and interdependencies, as demonstrated for diatoms [42].

Macroalgal-Bacterial Interactions

Ulva relies on interactions with bacteria for both the settlement its zoospores [43] and the morphogenesis of its thallus [10, 11]. This close association with bacteria, however, does not seem to have resulted in significantly higher levels of horizontal gene transfer (HGT). Using a phylogenomic pipeline to investigate the extent of HGT in the *Ulva* genome, we found 13 well-

supported cases of HGT of prokaryotic origin (Table S5). Although this number is not exceptionally high, it is remarkable that detected HGT events are followed by gene family expansion more than half the time. The most striking case is presented by Haem peroxidases belonging to the peroxidase-cyclooxygenase superfamily, of which *Ulva mutabilis* has 36 copies that arose following a single HGT event. Peroxidases, which are involved in scavenging H₂O₂, are part of *Ulva*'s antioxidant machinery and help it to cope with the environmental challenges common to intertidal habitats, such as excessive light, hypersalinity, and dehydration [16, 44]. Peroxidases may also have important functions in cell wall modification [45]; in plants, they have been demonstrated to anchor themselves to pectins and cross-link extensins, resulting in a stiffening of the primary cell wall. It is thus noteworthy that genes coding for extensins and pectin-like polysaccharides are very prominent in the *Ulva* genome (Data S1). Predictions of localization suggest that at least 21 of these peroxidases are extracellular, while a further five are predicted to be targeted to the mitochondrion.

A particularly interesting *Ulva*-bacterial interaction may involve the biosynthesis of siderophores for iron uptake. Pilot studies have recently revealed that bacteria tightly associated with *U. mutabilis* release unknown organic ligands that are capable of forming complexes with iron [46]. Secreted microbial siderophores become, therefore, part of the organic matter in the chemosphere and contribute to the recruitment of iron within the tripartite community of *U. mutabilis*. It was hypothesized that *Ulva* uses siderophores as public goods within a bacterial-algal mutualism, where heterotrophic bacteria are fed by the algae through the release of carbon sources. Genome mining for iron uptake genes suggests that *Ulva* can acquire iron, maintained in solution and made bioavailable by bacterial siderophores, via reduction by a ferric chelate reductase, re-oxidation by a multicopper ferroxidase, and finally uptake by a transferrin-like protein (Data S1).

Dimethylsulfoniopropionate Synthesis

DMSP has been identified as a major metabolite in *Ulva*. In addition to its role as an osmolyte and cryoprotectant, DMSP also appears to play a direct role in cross-kingdom signaling between *Ulva* and its associated bacteria [47]. *Roseovarius* sp. strain MS2 is chemotactically attracted to DMSP. Bacteria use the algal DMSP signal as a mechanism for detecting the presence of a photoautotrophic organism releasing various carbon sources such as glycerol [47]. In turn, *Roseovarius* sp. promotes the growth of *Ulva* by a cytokinin-like substance. DMSP works thus as an important chemical mediator for macroalgal-bacteria interactions [47]. Comparative genome analysis reveals genes with a putative function in biosynthesis, catabolism, and transport of DMSP.

The biosynthesis of DMSP in *Ulva* has already been demonstrated to follow an entirely different route from that in flowering plants [48]. In a four-step pathway, methionine is first transaminated to 4-methylthio-2-oxobutyrate (MTOB), then reduced to 4-methylthio-2-hydroxybutyrate (MTHB), and then methylated to give 4-dimethylsulfonio-2-hydroxybutyrate (DMSHB) (Figure 7A). Finally, the oxidative decarboxylation of DMSHB yields DMSP. The methylation of MTHB to DMSHB is only known to occur in association with DMSP synthesis and is thus considered

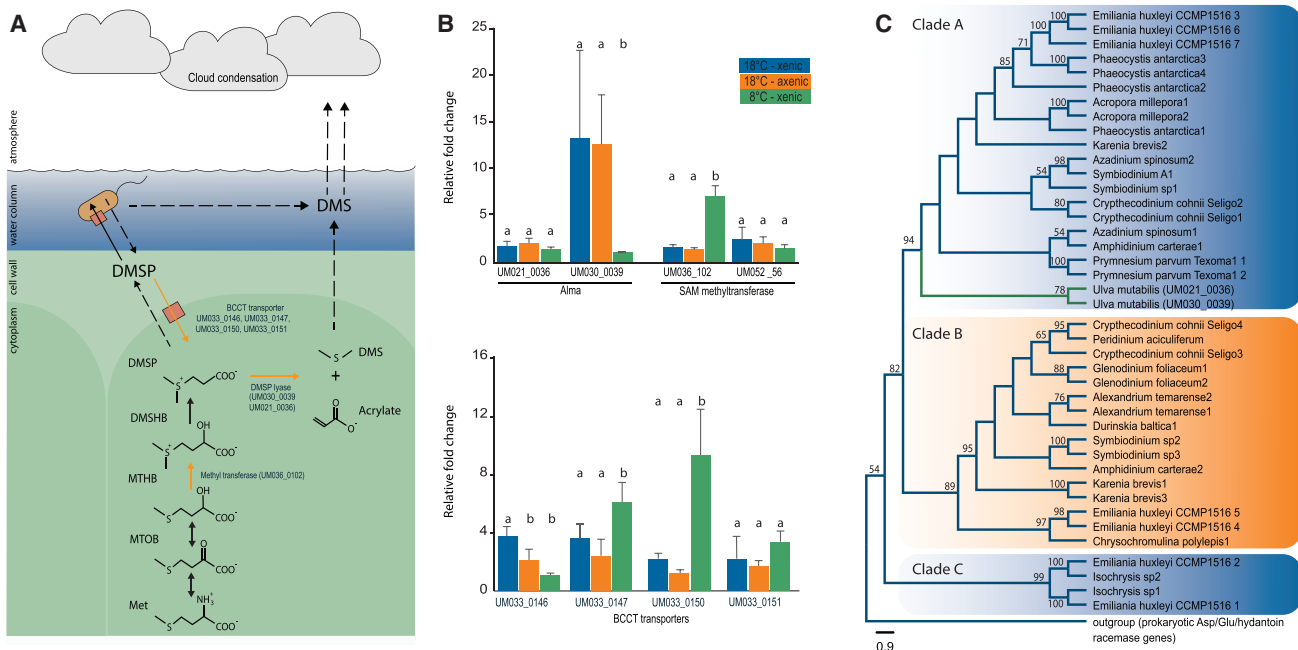


Figure 7. Biosynthesis, Transport, and Catabolism of DMSP

(A) Maintenance of DMSP concentration in *Ulva* is a combination of *de novo* synthesis by conversion of methionine [48], import from the environment putatively using BCCT transporters [49], and degradation into acrylate and DMS by DMSP lyases [50].

(B) Expression analysis (qPCR) of the *Alma* DMSP lyase homologues, putative S-adenosyl-L-methionine-dependent methyltransferases, and BCCT transporters in xenic and axenic *Ulva* at 18°C and 8°C. Results shown are based on four replicates, except UM030_0039, for which eight replicates were used. Significant expression values (Fisher’s post-hoc test) are indicated for each gene. Error bars represent standard deviation.

(C) Maximum likelihood phylogeny of the DMSP lyase genes, indicating lateral gene transfer of the *Alma* gene from the “chromalveolate” lineage.

See also Table S8.

expression values correlate with DMSP concentrations, which are significantly higher at 8°C (5.75 ± 1.8 mg/g FW) than at 18°C (3.14 ± 1.05 mg/g FW; Student’s *t* test $p < 0.001$, $n = 12$), consistent with a potential role for DMSP as a cryoprotectant. The expression of UM052_056, a SAM methyltransferase with homologs in volvocine algae, which was included as a control, was not increased. The combination of comparative analyses and expression data make UM036_0102 a credible candidate for the enzyme that mediates the methylation step in the biosynthesis of DMSP as an alternative to *DSYB* in eukaryotes.

Also relevant when considering DMSP synthesis are four putative BCCT-type family symporters/antiporters (IPR000060), which have been demonstrated to be involved in the import of DMSP in several bacteria [54]. In *Ulva*, which shifts from DMSP synthesis towards DMSP uptake under conditions of sulfur deficiency, a putative DMSP transporter has been shown to be a Na^+ /DMSP symporter, which points towards BCCT transporters [49]. Homologs of the putative *Ulva* BCCT transporters are also present in diatoms, some marine prasinophytes, and opisthokonts, but are notably absent from the fresh water Trebouxiophyceae and Chlorophyceae. Two out of four BCCT transporters are significantly up-regulated at low temperatures (UM033_147 and 150), while one is significantly downregulated (UM033_146) (Figure 7B).

Finally, the *Ulva* genome encodes two copies of a DMSP lyase, the enzyme responsible for forming DMS from DMSP (Figure 7A), which was originally identified in *Emiliania huxleyi* [50]. *Ulva* may thus regulate the chemoattraction of bacteria by the *de novo*

synthesis of DMSP and its decomposition to DMS through its endogenous DMSP lyase. The production of DMSP and DMS by *Ulva* [48], as well as the ecological implications for the natural sulfur cycle and climate regulation (e.g., cloud condensation), are an important topic of research. The involvement of a DMSP lyase in the production of DMS has been demonstrated in the past [55], but the enzymes remained unidentified. Furthermore, the production of DMS by *Ulva* rather than by associated bacteria has only recently been unequivocally demonstrated [47]. Phylogenetic analyses resolved two DMSP lyases that are present in *U. mutabilis* in a clade with several haptophytes (including *Alma* 3, 6, and 7 of *Emiliania huxleyi*) and dinoflagellates, but also with the lyases of the scleractinian coral *Acropora* (Figure 7C). The most likely explanation for the presence of the *Alma* DMSP lyases in *Ulva*—the first reported in any green algal genome—would therefore be through HGT from the chromalveolate lineage rather than from bacteria. Of the two *Ulva* DMSP lyase copies, UM030_0039 was 13-fold downregulated at low temperatures (Figure 7B), while the expression of UM021_0036 did not vary significantly across treatments, which may indicate a function disconnected from temperature-responsive DMS formation.

Conclusion

Genome analysis of *U. mutabilis* reveals several key insights into the biology of green seaweeds. Most importantly, we demonstrate that *Ulva*’s long independent evolution from a unicellular and

freshwater ancestral chlorophyte has resulted in marked changes in the genes underlying the most important aspects of the species' biology (e.g., cell-cycle control). Although the unicellular-multicellular transition in volvocine algae relies on substantially different proximate causes, such as co-option of the RB cell-cycle pathway, interesting parallels can be drawn between expansions in the volvocine algae and the expansions of *Ulva*'s ECM-related gene families, especially given their putative role in environmental signaling. Additional ongoing advances in the precision and efficiency of reverse genetic and genome-editing techniques, combined with *Ulva*'s experimental tractability and ease of clonal haploid growth under laboratory conditions, make *Ulva* an exciting model organism for the study of the marine green seaweeds. *Ulva* is increasingly used as a crop in seaweed aquaculture, and its sustainable and biosecure exploitation and domestication will benefit from the identification of ecotypic genetic variation—most immediately in identifying the traits that underlie bloom formation. For example, the comparison of bloom- and non-bloom-forming *Ulva* species may assist our understanding of the molecular mechanisms that underpin growth and reproduction in response to environmental conditions. Furthermore, expanding comparative genomics to giant-celled green seaweeds (e.g. *Acetabularia*, *Caulerpa*, and *Cladophora*) has the potential to shed light on a range of curious macroscopic organismal architectures that do not rely on multicellularity for morphological patterning. Lastly, the reliance of *Ulva* on bacterial cues for growth and morphogenesis makes the species an exciting model to study the evolution of cross-kingdom signaling in the marine environment.

STAR★METHODS

Detailed methods are provided in the online version of this paper and include the following:

- KEY RESOURCES TABLE
- CONTACT FOR REAGENT AND RESOURCE SHARING
- EXPERIMENTAL MODEL AND SUBJECT DETAILS
- METHOD DETAILS
 - DNA and RNA extraction and library construction
 - Genome sequencing and assembly
 - De novo repeat finding and repeat masking
 - Gene prediction
 - Genome completeness
 - Comparative genomic analyses
 - Horizontal gene transfer
 - Phytohormone bioassay and measurements
 - Measurement of DMSP and qPCR
- QUANTIFICATION AND STATISTICAL ANALYSIS
- DATA AND SOFTWARE AVAILABILITY

SUPPLEMENTAL INFORMATION

Supplemental Information includes five figures, eight tables, and one data file and can be found with this article online at <https://doi.org/10.1016/j.cub.2018.08.015>.

ACKNOWLEDGMENTS

Research support was provided by NERC grant NBAF925 and BBSRC grant BB:K020552 (to C.A.M. and J.H.B.), UGent Special Research Fund BOF/

01J04813 (to O.D.C. and K.V.), BOF/GOA 01G01715 (to K.V. and E.V), and BOF/01SC2316 (to X.L.) with infrastructure funded by EMBRC Belgium—FWO project GOH3817N (to O.D.C.), EU Horizon2020 Marie Curie ITN ALFF-Project 642575 (to C.M.G., O.D.C., T.W., G.C., and Y.V.d.P.), German Research Foundation CRC ChemBioSys 1127 (to T.W., J. Boesger, M.K., G.C., and L.L.), Postdoctoral Fellowship Grant of the Research Foundation—Flanders (to J. Blomme—project 12T3418N), BBSRC-funded MIBTP PhD rotation project (to R.C. and J.C.C.), United States Department of Energy DE-EE0003373/001 (to D.B.), and National Science Foundation IGERT for Renewable and Sustainable Fuels program 0903675 (to F.F.). M.H. is research associate of the FNRS. We thank Dr. Severin Sasso (University Jena) for providing T.W. with the real-time PCR detection system. This publication is based upon work from COST Action FA1406 PHYCOMORPH (to B.C., J.C.C., J.H.B., O.D.C., S.A.R., and T.W.), supported by COST (European Cooperation in Science and Technology).

AUTHOR CONTRIBUTIONS

J.H.B., O.D.C., T.W., K.V., L.S., and Y.V.d.P. designed research; O.D.C., S.-M.K., K.A.B., J. Blomme, F.F., M.K., E.V., L.V., E.A., J. Boesger, G.C., B.C., R.C., A.D.C., N.F.-P., C.M.G., M.H., L.L., F.L., X.L., Z.A.P., M.V.B., P.K.I.W., D.B., J.C.C., S.A.R., D.V.D.S., L.S., T.W., and J.H.B. performed research; S.-M.K., K.A.B., M.K., E.V., L.V., E.A., G.C., L.L., X.L., M.V.B., N.F.-P., P.K.I.W., L.S., and J.H.B. contributed new reagents/analytic tools; O.D.C., S.-M.K., K.A.B., J. Blomme, F.F., M.K., E.V., L.V., B.C., R.C., A.D.C., M.H., F.L., Z.A.P., J.A.R., D.B., J.C.C., S.A.R., D.V.D.S., A.V., L.S., K.V., T.W. and J.H.B. analyzed data; A.D.C., J. Blomme, G.C., S.D., L.L., L.V., and X.L. prepared samples; and O.D.C., S.-M.K., K.A.B., F.L., C.A.M., D.B., J.C.C., S.A.R., D.V.D.S., A.V., L.S., K.V., T.W., J.H.B., K.V., and Y.V.d.P. wrote the paper.

DECLARATION OF INTERESTS

The authors declare no competing interests.

Received: April 3, 2018

Revised: June 21, 2018

Accepted: August 3, 2018

Published: September 13, 2018

REFERENCES

1. Seb e-Pedr s, A., Degnan, B.M., and Ruiz-Trillo, I. (2017). The origin of Metazoa: a unicellular perspective. *Nat. Rev. Genet.* 18, 498–512.
2. Rensing, S.A. (2016). (Why) Does Evolution Favour Embryogenesis? *Trends Plant Sci.* 21, 562–573.
3. Ju, C., Van de Poel, B., Cooper, E.D., Thierer, J.H., Gibbons, T.R., Delwiche, C.F., and Chang, C. (2015). Conservation of ethylene as a plant hormone over 450 million years of evolution. *Nat. Plants* 1.
4. Umen, J.G., and Olson, B.J.S.C. (2012). Genomics of Volvocine Algae. In *Genomic insights into the biology of algae, Volume 64*, G. Piganeau, ed. (Academic Press), pp. 185–243.
5. Featherston, J., Arakaki, Y., Hanschen, E.R., Ferris, P.J., Michod, R.E., Olson, B.J.S.C., Nozaki, H., and Durand, P.M. (2018). The 4-Celled *Tetrahymena socialis* Nuclear Genome Reveals the Essential Components for Genetic Control of Cell Number at the Origin of Multicellularity in the Volvocine Lineage. *Mol. Biol. Evol.* 35, 855–870.
6. Prochnik, S.E., Umen, J., Nedelcu, A.M., Hallmann, A., Miller, S.M., Nishii, I., Ferris, P., Kuo, A., Mitros, T., Fritz-Laylin, L.K., et al. (2010). Genomic analysis of organismal complexity in the multicellular green alga *Volvox carteri*. *Science* 329, 223–226.
7. Hanschen, E.R., Marriage, T.N., Ferris, P.J., Hamaji, T., Toyoda, A., Fujiyama, A., Neme, R., Noguchi, H., Minakuchi, Y., Suzuki, M., et al. (2016). The *Gonium pectorale* genome demonstrates co-option of cell cycle regulation during the evolution of multicellularity. *Nat. Commun.* 7, 11370.

8. Leliaert, F., Smith, D.R., Moreau, H., Herron, M.D., Verbruggen, H., Delwiche, C., and De Clerck, O. (2012). Phylogeny and molecular evolution of the green algae. *Crit. Rev. Plant Sci.* *31*, 1–46.
9. Mine, I., Menzel, D., and Okuda, K. (2008). Morphogenesis in giant-celled algae. *Int. Rev. Cell Mol. Biol.* *266*, 37–83.
10. Wichard, T., Charrier, B., Mineur, F., Bothwell, J.H., Clerck, O.D., and Coates, J.C. (2015). The green seaweed *Ulva*: a model system to study morphogenesis. *Front. Plant Sci.* *6*, 72.
11. Spoerner, M., Wichard, T., Bachhuber, T., Stratmann, J., and Oertel, W. (2012). Growth and thallus morphogenesis of *Ulva mutabilis* (Chlorophyta) depends on a combination of two bacterial species excreting regulatory factors. *J. Phycol.* *48*, 1433–1447.
12. Matsuo, Y., Imagawa, H., Nishizawa, M., and Shizuri, Y. (2005). Isolation of an algal morphogenesis inducer from a marine bacterium. *Science* *307*, 1598.
13. Oertel, W., Wichard, T., and Weissgerber, A. (2015). Transformation of *Ulva mutabilis* (Chlorophyta) by vector plasmids integrating into the genome. *J. Phycol.* *51*, 963–979.
14. Smetacek, V., and Zingone, A. (2013). Green and golden seaweed tides on the rise. *Nature* *504*, 84–88.
15. Bolton, J.J., Cyrus, M.D., Brand, M.J., Joubert, M., and Macey, B.M. (2016). Why grow *Ulva*? Its potential role in the future of aquaculture. *Perspect. Phycol.* *3*, 113–120.
16. Zhang, X., Ye, N., Liang, C., Mou, S., Fan, X., Xu, J., Xu, D., and Zhuang, Z. (2012). De novo sequencing and analysis of the *Ulva linza* transcriptome to discover putative mechanisms associated with its successful colonization of coastal ecosystems. *BMC Genomics* *13*, 565.
17. Yamazaki, T., Ichihara, K., Suzuki, R., Oshima, K., Miyamura, S., Kuwano, K., Toyoda, A., Suzuki, Y., Sugano, S., Hattori, M., and Kawano, S. (2017). Genomic structure and evolution of the mating type locus in the green seaweed *Ulva partita*. *Sci. Rep.* *7*, 11679.
18. Ranjan, A., Townsley, B.T., Ichihashi, Y., Sinha, N.R., and Chitwood, D.H. (2015). An intracellular transcriptomic atlas of the giant coenocyte *Caulerpa taxifolia*. *PLoS Genet.* *11*, e1004900.
19. Føyn, B. (1958). Über die Sexualität und den Generationswechsel von *Ulva mutabilis*. *Arch. Protistenkd.* *102*, 473–480.
20. Løvlie, A. (1978). On the genetic control of cell cycles during morphogenesis in *Ulva mutabilis*. *Dev. Biol.* *64*, 164–177.
21. Khanna, R., Kronmiller, B., Maszke, D.R., Coupland, G., Holm, M., Mizuno, T., and Wu, S.-H. (2009). The *Arabidopsis* B-box zinc finger family. *Plant Cell* *21*, 3416–3420.
22. Harashima, H., Dissmeyer, N., and Schnittger, A. (2013). Cell cycle control across the eukaryotic kingdom. *Trends Cell Biol.* *23*, 345–356.
23. Lang, D., Weiche, B., Timmerhaus, G., Richardt, S., Riaño-Pachón, D.M., Corrêa, L.G., Reski, R., Mueller-Roeber, B., and Rensing, S.A. (2010). Genome-wide phylogenetic comparative analysis of plant transcriptional regulation: a timeline of loss, gain, expansion, and correlation with complexity. *Genome Biol. Evol.* *2*, 488–503.
24. Cockram, J., Thiel, T., Steuernagel, B., Stein, N., Taudien, S., Bailey, P.C., and O'Sullivan, D.M. (2012). Genome dynamics explain the evolution of flowering time CCT domain gene families in the Poaceae. *PLoS ONE* *7*, e45307.
25. Putterill, J., Robson, F., Lee, K., Simon, R., and Coupland, G. (1995). The CONSTANS gene of *Arabidopsis* promotes flowering and encodes a protein showing similarities to zinc finger transcription factors. *Cell* *80*, 847–857.
26. Strayer, C., Oyama, T., Schultz, T.F., Raman, R., Somers, D.E., Más, P., Panda, S., Kreps, J.A., and Kay, S.A. (2000). Cloning of the *Arabidopsis* clock gene *TOC1*, an autoregulatory response regulator homolog. *Science* *289*, 768–771.
27. Liu, J., Shen, J., Xu, Y., Li, X., Xiao, J., and Xiong, L. (2016). *Ghd2*, a CONSTANS-like gene, confers drought sensitivity through regulation of senescence in rice. *J. Exp. Bot.* *67*, 5785–5798.
28. Corellou, F., Schwartz, C., Motta, J.-P., Djouani-Tahri, B., Sanchez, F., and Bouget, F.Y. (2009). Clocks in the green lineage: comparative functional analysis of the circadian architecture of the picoeukaryote *ostreococcus*. *Plant Cell* *21*, 3436–3449.
29. Serrano, G., Herrera-Palau, R., Romero, J.M., Serrano, A., Coupland, G., and Valverde, F. (2009). *Chlamydomonas* CONSTANS and the evolution of plant photoperiodic signaling. *Curr. Biol.* *19*, 359–368.
30. Lang, D., and Rensing, S.A. (2015). The Evolution of Transcriptional Regulation in the Viridiplantae and its Correlation with Morphological Complexity. In *Evolutionary Transitions to Multicellular Life: Principles and mechanisms*, I. Ruiz-Trillo, and A.M. Nedelcu, eds. (Dordrecht: Springer Netherlands), pp. 301–333.
31. Holzinger, A., Herburger, K., Kaplan, F., and Lewis, L.A. (2015). Desiccation tolerance in the chlorophyte green alga *Ulva compressa*: does cell wall architecture contribute to ecological success? *Planta* *242*, 477–492.
32. Daher, F.B., and Braybrook, S.A. (2015). How to let go: pectin and plant cell adhesion. *Front. Plant Sci.* *6*, 523.
33. Green, J.L., Kuntz, S.G., and Sternberg, P.W. (2008). Ror receptor tyrosine kinases: orphans no more. *Trends Cell Biol.* *18*, 536–544.
34. Wheeler, G.L., Miranda-Saavedra, D., and Barton, G.J. (2008). Genome analysis of the unicellular green alga *Chlamydomonas reinhardtii* Indicates an ancient evolutionary origin for key pattern recognition and cell-signaling protein families. *Genetics* *179*, 193–197.
35. Bessa Pereira, C., Bocková, M., Santos, R.F., Santos, A.M., Martins de Araújo, M., Oliveira, L., Homola, J., and Carmo, A.M. (2016). The Scavenger Receptor SSc5D Physically Interacts with Bacteria through the SRCR-Containing N-Terminal Domain. *Front. Immunol.* *7*, 416.
36. Bowdish, D.M., and Gordon, S. (2009). Conserved domains of the class A scavenger receptors: evolution and function. *Immunol. Rev.* *227*, 19–31.
37. Zimmermann, G., Bäumllein, H., Mock, H.-P., Himmelbach, A., and Schweizer, P. (2006). The multigene family encoding germin-like proteins of barley. Regulation and function in Basal host resistance. *Plant Physiol.* *142*, 181–192.
38. Hallmann, A., Amon, P., Godl, K., Heitzer, M., and Sumper, M. (2001). Transcriptional activation by the sexual pheromone and wounding: a new gene family from *Volvox* encoding modular proteins with (hydroxy) proline-rich and metalloproteinase homology domains. *Plant J.* *26*, 583–593.
39. Provasoli, L. (1958). Effect of plant hormones on *Ulva*. *Biol. Bull.* *114*, 375–384.
40. Gupta, V., Kumar, M., Brahmabhatt, H., Reddy, C.R., Seth, A., and Jha, B. (2011). Simultaneous determination of different endogenous plant growth regulators in common green seaweeds using dispersive liquid-liquid microextraction method. *Plant Physiol. Biochem.* *49*, 1259–1263.
41. Wang, C., Liu, Y., Li, S.-S., and Han, G.-Z. (2015). Insights into the origin and evolution of the plant hormone signaling machinery. *Plant Physiol.* *167*, 872–886.
42. Amin, S.A., Hmelo, L.R., van Tol, H.M., Durham, B.P., Carlson, L.T., Heal, K.R., Morales, R.L., Berthiaume, C.T., Parker, M.S., Djunaedi, B., et al. (2015). Interaction and signalling between a cosmopolitan phytoplankton and associated bacteria. *Nature* *522*, 98–101.
43. Joint, I., Tait, K., Callow, M.E., Callow, J.A., Milton, D., Williams, P., and Cámara, M. (2002). Cell-to-cell communication across the prokaryote-eukaryote boundary. *Science* *298*, 1207.
44. Sung, M.-S., Hsu, Y.-T., Hsu, Y.-T., Wu, T.-M., and Lee, T.-M. (2009). Hypersalinity and hydrogen peroxide upregulation of gene expression of antioxidant enzymes in *Ulva fasciata* against oxidative stress. *Mar. Biotechnol. (NY)* *11*, 199–209.
45. Passardi, F., Penel, C., and Dunand, C. (2004). Performing the paradoxical: how plant peroxidases modify the cell wall. *Trends Plant Sci.* *9*, 534–540.

46. Wichard, T. (2016). Identification of Metallophores and Organic Ligands in the Chemosphere of the Marine Macroalga *Ulva* (Chlorophyta) and at Land-Sea Interfaces. *Front. Mar. Sci.* 3, 131.
47. Kessler, R.W., Weiss, A., Kuegler, S., Hermes, C., and Wichard, T. (2018). Macroalgal-bacterial interactions: Role of dimethylsulfoniopropionate in microbial gardening by *Ulva* (Chlorophyta). *Mol. Ecol.* 27, 1808–1819.
48. Gage, D.A., Rhodes, D., Nolte, K.D., Hicks, W.A., Leustek, T., Cooper, A.J., and Hanson, A.D. (1997). A new route for synthesis of dimethylsulfoniopropionate in marine algae. *Nature* 387, 891–894.
49. Ito, T., Asano, Y., Tanaka, Y., and Takabe, T. (2011). REGULATION OF BIOSYNTHESIS OF DIMETHYLSULFONIOPROPIONATE AND ITS UPTAKE IN STERILE MUTANT OF ULVA PERTUSA (CHLOROPHYTA). *J. Phycol.* 47, 517–523.
50. Alcolombri, U., Ben-Dor, S., Feldmesser, E., Levin, Y., Tawfik, D.S., and Vardi, A. (2015). Identification of the algal dimethyl sulfide-releasing enzyme: A missing link in the marine sulfur cycle. *Science* 348, 1466–1469.
51. Curson, A.R.J., Williams, B.T., Pinchbeck, B.J., Sims, L.P., Martínez, A.B., Rivera, P.P.L., Kumaresan, D., Mercadé, E., Spurgin, L.G., Carrión, O., et al. (2018). DSYB catalyses the key step of dimethylsulfoniopropionate biosynthesis in many phytoplankton. *Nat. Microbiol.* 3, 430–439.
52. Curson, A.R., Liu, J., Bermejo Martínez, A., Green, R.T., Chan, Y., Carrión, O., Williams, B.T., Zhang, S.-H., Yang, G.-P., Bulman Page, P.C., et al. (2017). Dimethylsulfoniopropionate biosynthesis in marine bacteria and identification of the key gene in this process. *Nat. Microbiol.* 2, 17009.
53. Lyon, B.R., Lee, P.A., Bennett, J.M., DiTullio, G.R., and Janech, M.G. (2011). Proteomic analysis of a sea-ice diatom: salinity acclimation provides new insight into the dimethylsulfoniopropionate production pathway. *Plant Physiol.* 157, 1926–1941.
54. Sun, L., Curson, A.R.J., Todd, J.D., and Johnston, A.W.B. (2012). Diversity of DMSP transport in marine bacteria, revealed by genetic analyses. *Biogeochemistry* 110, 121–130.
55. Steinke, M., and Kirst, G.O. (1996). Enzymatic cleavage of dimethylsulfoniopropionate (DMSP) in cell-free extracts of the marine macroalga *Enteromorpha clathrata* (Roth) Grev. (Ulvales, Chlorophyta). *J. Exp. Mar. Biol. Ecol.* 201, 73–85.
56. Sterck, L., Billiau, K., Abeel, T., Rouzé, P., and Van de Peer, Y. (2012). ORCAE: online resource for community annotation of eukaryotes. *Nat. Methods* 9, 1041.
57. Wichard, T., and Oertel, W. (2010). Gametogenesis and gamete release of *Ulva mutabilis* and *Ulva lactuca* (Chlorophyta): Regulatory effects and chemical characterization of the “swarming inhibitor”. *J. Phycol.* 46, 248–259.
58. Gnerre, S., Maccallum, I., Przybylski, D., Ribeiro, F.J., Burton, J.N., Walker, B.J., Sharpe, T., Hall, G., Shea, T.P., Sykes, S., et al. (2011). High-quality draft assemblies of mammalian genomes from massively parallel sequence data. *Proc. Natl. Acad. Sci. USA* 108, 1513–1518.
59. Keller, O., Kollmar, M., Stanke, M., and Waack, S. (2011). A novel hybrid gene prediction method employing protein multiple sequence alignments. *Bioinformatics* 27, 757–763.
60. Hoff, K.J., Lange, S., Lomsadze, A., Borodovsky, M., and Stanke, M. (2016). BRAKER1: unsupervised RNA-Seq-based genome annotation with GeneMark-ET and AUGUSTUS. *Bioinformatics* 32, 767–769.
61. Waterhouse, R.M., Seppey, M., Simão, F.A., Manni, M., Ioannidis, P., Kliuchnikov, G., Kriventseva, E.V., and Zdobnov, E.M. (2017). BUSCO applications from quality assessments to gene prediction and phylogenomics. *Mol. Biol. Evol.* <https://doi.org/10.1093/molbev/msx1319>.
62. Koren, S., Walenz, B.P., Berlin, K., Miller, J.R., Bergman, N.H., and Phillippy, A.M. (2017). Canu: scalable and accurate long-read assembly via adaptive *k*-mer weighting and repeat separation. *Genome Res.* 27, 722–736.
63. Veeckman, E., Ruttink, T., and Vandepoele, K. (2016). Are we there yet? Reliably estimating the completeness of plant genome sequences. *Plant Cell* 28, 1759–1768.
64. Buchfink, B., Xie, C., and Huson, D.H. (2015). Fast and sensitive protein alignment using DIAMOND. *Nat. Methods* 12, 59–60.
65. Haas, B.J., Salzberg, S.L., Zhu, W., Pertea, M., Allen, J.E., Orvis, J., White, O., Buell, C.R., and Wortman, J.R. (2008). Automated eukaryotic gene structure annotation using EVIDENCEModeler and the Program to Assemble Spliced Alignments. *Genome Biol.* 9, R7.
66. Slater, G.S., and Birney, E. (2005). Automated generation of heuristics for biological sequence comparison. *BMC Bioinformatics* 6, 31.
67. Gouzy, J., Carrere, S., and Schiex, T. (2009). FrameDP: sensitive peptide detection on noisy matured sequences. *Bioinformatics* 25, 670–671.
68. Kim, D., Langmead, B., and Salzberg, S.L. (2015). HISAT: a fast spliced aligner with low memory requirements. *Nat. Methods* 12, 357–360.
69. Proost, S., Fostier, J., De Witte, D., Dhoedt, B., Demeester, P., Van de Peer, Y., and Vandepoele, K. (2012). i-ADHoRe 3.0—fast and sensitive detection of genomic homology in extremely large data sets. *Nucleic Acids Res.* 40, e11.
70. Nawrocki, E.P., and Eddy, S.R. (2013). Infernal 1.1: 100-fold faster RNA homology searches. *Bioinformatics* 29, 2933–2935.
71. Jones, P., Binns, D., Chang, H.-Y., Fraser, M., Li, W., McAnulla, C., McWilliam, H., Maslen, J., Mitchell, A., Nuka, G., et al. (2014). InterProScan 5: genome-scale protein function classification. *Bioinformatics* 30, 1236–1240.
72. Nguyen, L.-T., Schmidt, H.A., von Haeseler, A., and Minh, B.Q. (2015). IQ-TREE: a fast and effective stochastic algorithm for estimating maximum-likelihood phylogenies. *Mol. Biol. Evol.* 32, 268–274.
73. Zimin, A.V., Marçais, G., Puiu, D., Roberts, M., Salzberg, S.L., and Yorke, J.A. (2013). The MaSuRCA genome assembler. *Bioinformatics* 29, 2669–2677.
74. Bosi, E., Donati, B., Galardini, M., Brunetti, S., Sagot, M.-F., Lió, P., Crescenzi, P., Fani, R., and Fondi, M. (2015). MeDuSa: a multi-draft based scaffolder. *Bioinformatics* 31, 2443–2451.
75. Edgar, R.C. (2004). MUSCLE: multiple sequence alignment with high accuracy and high throughput. *Nucleic Acids Res.* 32, 1792–1797.
76. Emms, D.M., and Kelly, S. (2015). OrthoFinder: solving fundamental biases in whole genome comparisons dramatically improves orthogroup inference accuracy. *Genome Biol.* 16, 157.
77. Li, L., Stoeckert, C.J., Jr., and Roos, D.S. (2003). OrthoMCL: identification of ortholog groups for eukaryotic genomes. *Genome Res.* 13, 2178–2189.
78. Felsenstein, J. (2005). PHYLIP: Phylogenetic inference program, version 3.6 (Seattle: University of Washington).
79. Vandepoele, K., Van Bel, M., Richard, G., Van Landeghem, S., Verhelst, B., Moreau, H., Van de Peer, Y., Grimsley, N., and Piganeau, G. (2013). pico-PLAZA, a genome database of microbial photosynthetic eukaryotes. *Environ. Microbiol.* 15, 2147–2153.
80. Walker, B.J., Abeel, T., Shea, T., Priest, M., Abouelliel, A., Sakthikumar, S., Cuomo, C.A., Zeng, Q., Wortman, J., Young, S.K., and Earl, A.M. (2014). Pilon: an integrated tool for comprehensive microbial variant detection and genome assembly improvement. *PLoS ONE* 9, e112963.
81. Stamatakis, A. (2014). RAxML version 8: a tool for phylogenetic analysis and post-analysis of large phylogenies. *Bioinformatics* 30, 1312–1313.
82. Smit, A., Hubley, R., and Green, P. (2015). RepeatMasker Open (Institute for Systems Biology).
83. Smit, A., and Hubley, R. (2008). RepeatModeler (Institute for Systems Biology).
84. Shao, M., and Kingsford, C. (2017). Accurate assembly of transcripts through phase-preserving graph decomposition. *Nat. Biotechnol.* 35, 1167–1169.
85. Simpson, J.T. (2014). Exploring genome characteristics and sequence quality without a reference. *Bioinformatics* 30, 1228–1235.

86. Boetzer, M., Henkel, C.V., Jansen, H.J., Butler, D., and Pirovano, W. (2011). Scaffolding pre-assembled contigs using SSPACE. *Bioinformatics* *27*, 578–579.
87. Enright, A.J., Van Dongen, S., and Ouzounis, C.A. (2002). An efficient algorithm for large-scale detection of protein families. *Nucleic Acids Res.* *30*, 1575–1584.
88. Grabherr, M.G., Haas, B.J., Yassour, M., Levin, J.Z., Thompson, D.A., Amit, I., Adiconis, X., Fan, L., Raychowdhury, R., Zeng, Q., et al. (2011). Full-length transcriptome assembly from RNA-Seq data without a reference genome. *Nat. Biotechnol.* *29*, 644–652.
89. Schattner, P., Brooks, A.N., and Lowe, T.M. (2005). The tRNAscan-SE, snoscan and snoGPS web servers for the detection of tRNAs and snoRNAs. *Nucleic Acids Res.* *33*, W686–W689.
90. Capella-Gutiérrez, S., Silla-Martínez, J.M., and Gabaldón, T. (2009). trimAl: a tool for automated alignment trimming in large-scale phylogenetic analyses. *Bioinformatics* *25*, 1972–1973.
91. Hare, E.E., and Johnston, J.S. (2012). Genome size determination using flow cytometry of propidium iodide-stained nuclei. *Methods Mol. Biol.* *772*, 3–12.
92. Suzek, B.E., Wang, Y., Huang, H., McGarvey, P.B., and Wu, C.H.; UniProt Consortium (2015). UniRef clusters: a comprehensive and scalable alternative for improving sequence similarity searches. *Bioinformatics* *31*, 926–932.
93. Matasci, N., Hung, L.-H., Yan, Z., Carpenter, E.J., Wickett, N.J., Mirarab, S., Nguyen, N., Warnow, T., Ayyampalayam, S., Barker, M., et al. (2014). Data access for the 1,000 Plants (1KP) project. *Gigascience* *3*, 17.
94. Wilhelmsson, P.K.I., Mühlich, C., Ullrich, K.K., and Rensing, S.A. (2017). Comprehensive Genome-Wide Classification Reveals That Many Plant-Specific Transcription Factors Evolved in Streptophyte Algae. *Genome Biol. Evol.* *9*, 3384–3397.
95. Camacho, C., Coulouris, G., Avagyan, V., Ma, N., Papadopoulos, J., Bealer, K., and Madden, T.L. (2009). BLAST+: architecture and applications. *BMC Bioinformatics* *10*, 421.
96. Qiu, H., Price, D.C., Weber, A.P., Reeb, V., Yang, E.C., Lee, J.M., Kim, S.Y., Yoon, H.S., and Bhattacharya, D. (2013). Adaptation through horizontal gene transfer in the cryptoendolithic red alga *Galdieria phlegrea*. *Curr. Biol.* *23*, R865–R866.
97. Matsuura, T., Mori, I.C., Ikeda, Y., Hirayama, T., and Mikami, K. (2018). Comprehensive phytohormone quantification in the red alga *Pyropia yezoensis* by liquid chromatography–mass spectrometry. In *Protocols for Macroalgae Research*, B. Charrier, T. Wichard, and C.R.K. Reddy, eds. (Boca Raton: CRC Press, Francis & Taylor Group).
98. Hu, Y., Depaepe, T., Smet, D., Hoyerova, K., Klíma, P., Cuypers, A., Cutler, S., Buyst, D., Morreel, K., Boerjan, W., et al. (2017). ACCERBATIN, a small molecule at the intersection of auxin and reactive oxygen species homeostasis with herbicidal properties. *J. Exp. Bot.* *68*, 4185–4203.
99. Vandesompele, J., De Preter, K., Pattyn, F., Poppe, B., Van Roy, N., De Paepe, A., and Speleman, F. (2002). Accurate normalization of real-time quantitative RT-PCR data by geometric averaging of multiple internal control genes. *Genome Biol.* *3*.
100. R Development Core Team. (2018). R: A Language and Environment for Statistical Computing (R Foundation for Statistical Computing).

STAR★METHODS

KEY RESOURCES TABLE

REAGENT or RESOURCE	SOURCE	IDENTIFIER
Critical Commercial Assays		
TruSeq DNA PCR-Free Library Preparation Kit	Illumina	Catalog #: FC-121-3001
Nextera Mate Pair Sample Preparation Kit	Illumina	Catalog #: FC-132-1001
ScriptSeq v2 RNA-Seq Library Preparation Kit	Illumina	Catalog #: SSV21106
Deposited Data		
Bioproject <i>Ulva mutabilis</i> : raw and analyzed sequence data	EMBL BioProject	PRJEB25750
ORCAE Online annotation platform	ORCAE [56]	http://bioinformatics.psb.ugent.be/orcae/overview/Ulvmu
Genome assembly		
DNA reads: 2 x 250 bp, insert size 350 bp [Illumina MiSeq]	EMBL	ERR2447202
DNA reads: 2 x 250 bp, insert size 550 bp [Illumina MiSeq]	EMBL	ERR2447203
DNA reads: 2 x 125 bp, insert size 5 kb [Illumina HiSeq 2500]	EMBL	ERR2486500
DNA reads: 2 x 125 bp, insert size 10 kb [Illumina HiSeq 2500]	EMBL	ERR2486501
RNA-seq reads: 2x125 bp [Illumina HiSeq 2500]	EMBL	ERR2722103, ERR2722112, ERR2722113, ERR2722114
RNA-seq reads: 150 bp [Illumina NextSeq 550]	EMBL	ERR2722121 to ERR2722135
PacBio RSII [P6 chemistry]	EMBL	ERR2721964, ERR2721965, ERR2721966, ERR2721967, ERR2721968
Experimental Models: Organisms/Strains		
<i>Ulva mutabilis</i> Føyn (wildtype and slender strains)	[57]	Friedrich Schiller University Jena, Germany
<i>Roseovarius</i> sp. MS2	[11]	Friedrich Schiller University Jena, Germany
<i>Maribacter</i> sp. MS6	[11]	Friedrich Schiller University Jena, Germany
Software and Algorithms		
Genome size estimation	ALLPATHS-LG [58]	http://software.broadinstitute.org/allpaths-lg/blog/?page_id=12
Gene prediction	Augustus-PPX [59]	http://bioinf.uni-greifswald.de/augustus/
Assembly polishing	Arrow (v2.2.1) (SMRT Link v5.0.1.9585)	https://www.pacb.com/support/software-downloads/
Gene prediction	BRAKER1 (v1.9) [60]	http://exon.gatech.edu/braker1.html
Genome completeness	BUSCO (v3.0.2b) [61]	https://gitlab.com/ezlab/busco
Genome assembly	Canu (v1.6) [62]	https://github.com/marbl/canu
Genome completeness	Core gene family analysis [63]	ftp://ftp.psb.ugent.be/pub/plaza/plaza_public_02_5/coreGF
Protein alignment prior to gene prediction	Diamond (v0.9.18) [64]	https://github.com/bbuchfink/diamond
Gene prediction	EvidenceModeler [65]	https://evidencemodeler.github.io/
Gene prediction	Exonerate (v2.2.0) [66]	https://www.ebi.ac.uk/about/vertebrate-genomics/software/exonerate
Reading frame correction	FrameDP (v1.2.2) [67]	https://iant.toulouse.inra.fr/FrameDP/

(Continued on next page)

Continued

REAGENT or RESOURCE	SOURCE	IDENTIFIER
RNA-seq mapping	HISAT2 (v2.0.5) [68]	https://ccb.jhu.edu/software/hisat2/index.shtml
Detection of collinear regions	i-ADHoRe (v3.0.01) [69]	http://bioinformatics.psb.ugent.be/beg/tools/i-adhore30
Prediction of non-coding RNA	Infernal [70]	http://eddylab.org/infernal/
Functional annotation	InterProScan (v5.27-66) [71]	https://www.ebi.ac.uk/interpro/
Maximum likelihood tree calculation	IQtree (v1.4.3) [72]	http://www.iqtree.org/
Genome assembly	MaSuRCA (v3.2.3) [73]	https://github.com/alekseymzin/masurca
Contig scaffolding	MEDUSA [74]	https://github.com/combogenomics/medusa
Sequence alignment	Muscle (v3.8.31) [75]	https://www.ebi.ac.uk/Tools/msa/muscle/
Gene family prediction	OrthoFinder (v2.1.2) [76]	https://github.com/davidemms/OrthoFinder
Gene family prediction	OrthoMCL [77]	http://orthomcl.org/orthomcl/
Gene prediction	PASA [65]	https://github.com/PASAPipeline/PASAPipeline
Long-read mapping	pbalgn (v0.3.1) (SMRT Link v5.0.1.9585)	https://www.pacb.com/support/software-downloads/
Gene family loss/gain analysis	PHYLIP (Dollop) [78]	http://evolution.genetics.washington.edu/phylip.html
Comparative genomics	Pico-PLAZA (v2.0) [79]	https://bioinformatics.psb.ugent.be/plaza/versions/pico-plaza/
Assembly polishing	Pilon (v1.20) [80]	https://github.com/broadinstitute/pilon
Maximum likelihood tree calculation	RAxML (v8.2.4) [81]	https://sco.h-its.org/exelixis/web/software/raxml/index.html
Repetitive DNA-motif masking	RepeatMasker (v4.0.7) [82]	https://github.com/rmhubble/RepeatMasker
Repetitive DNA-motif identification	RepeatModeler (1.0.8) [83]	https://github.com/rmhubble/RepeatModeler
Reference-based transcriptome assembly	Scallop (v0.10.2) [84]	https://github.com/Kingsford-Group/scallop
Genome size estimation	SGA PreQC [85]	https://github.com/jts/sga
Contig scaffolding	SSPACE (v3.0) [86]	https://github.com/nsoranzo/sspace_basic
Gene family prediction	TribeMCL [87]	https://micans.org/mcl/
Transcriptome assembly	Trinity v2.4.0 [88]	https://github.com/trinityrnaseq/trinityrnaseq
tRNA identification	tRNAscan-SE (v1.31) [89]	http://lowelab.ucsc.edu/tRNAscan-SE/
Alignment curation	Trimal (v1.2) [90]	http://trimal.cgenomics.org/

CONTACT FOR REAGENT AND RESOURCE SHARING

Further information and requests for resources and reagents should be directed to and will be fulfilled by the Lead Contact, Olivier De Clerck (olivier.declerck@ugent.be).

EXPERIMENTAL MODEL AND SUBJECT DETAILS

The *U. mutabilis* strain sequenced, a wildtype gametophyte of mating type minus (wt-G(mt-) (gametophyte); ([mt-]; G/PS- swi⁺; mut-; RS140⁺; RS180⁺)) was initially isolated from Ria Formosa, southern Portugal, by B. Føyn [13, 19]. An additional haploid strain, *slender*, a spontaneous mutant derived from the original collection, was selected to complement the available transcriptomes because of its fast-growing nature and the ease with which thalli can be induced for gamete formation. Strains of *U. mutabilis* are primarily maintained at the Friedrich-Schiller-Universität Jena. Gametophytes were raised parthenogenetically from unmated gametes in *Ulva* Culture Medium (UCM without antibiotics) in the presence of bacterial symbionts *Roseovarius* sp. MS2 (Genbank: EU359909) and *Maribacter* sp. MS6 (Genbank: EU359911) to secure normal thallus morphogenesis. Bacterial strains are cultivated in marine broth medium (Roth, Germany). Algae were cultured at 20°C, under long day light conditions (L/D 17:7) consisting of 60–120 μmol photons·m⁻²·s⁻¹ (50% GroLux, 50% day-light fluorescent tubes; OSRAM, München, Germany), without aeration.

METHOD DETAILS

DNA and RNA extraction and library construction

DNA for sequencing was prepared from axenic gametes. For mate pair libraries adult, non-axenic *Ulva* tissue was used. DNA extraction was performed using a CTAB protocol. The PacBio library was prepared using P6-C4.0 chemistry with size selection using a 0.75% cassette on a Blue Pippin instrument with a lower cutoff of 8 kb based on the Pacific Biosciences 20kb template protocol (ref 100-286-000-08). Libraries for short reads and mate pairs were constructed using the TruSeq DNA PCR-Free Library Preparation Kit and the Nextera Mate Pair Sample Preparation Kit, respectively (Illumina, San Diego, CA). Total RNA was isolated from vegetative adult tissue, tissue in the process of gamete formation as well as gametes using the RNeasy Mini Kit (Qiagen). cDNA libraries were constructed using the ScriptSeq v2 RNA-Seq Library Preparation Kit.

Genome sequencing and assembly

Sequencing

Genomic DNA was sheared to produce fragments of 350 to 550 bp and sequenced on a MiSeq2000 (2x250 bp PE reads). Mate-pair libraries were sequenced on an Illumina HiSeq 2500 (2x125 bp reads). The PacBio libraries were sequenced on a PacBio RSII instrument (five SMRTCells P6-C4 chemistry). RNA libraries were sequenced on one lane of Illumina HiSeq 2500 (2x125 bp PE reads) and one run of NextSeq 550 (1x150 bp SE reads). Table S6 presents an overview of the sequenced libraries.

Estimation of genome size

Both k-mer analysis and flow cytometry experiments were used to gauge the genome size of *Ulva mutabilis* (wild-type). Based on the concatenated Illumina paired-end libraries the genome size was estimated 93.6 Mbp by SGA PreQC [85] with default k-mer size 31 and 104.5 Mbp by the estimating process in ALLPATHS-LG [58] with k-mer size 25. For flow cytometry estimates, *Ulva mutabilis* nuclei were stained together with nuclei of the standard (*Arabidopsis thaliana*) and relative fluorescence was used to calculate the genome size as described by Hare & Johnston [91]. Fluorescence emission was collected using the S3 Cell Sorter (BIO-RAD). The flow cytometry measurements showed an estimated genome size of 100.2 ± 3.6 Mbp (mean \pm standard error of four measurements).

Genome assembly

PacBio reads (6.9 Gbp) were assembled using Canu [62] resulting in a 98.4 Mbp assembly in 1,119 contigs. The 30x of the longest corrected reads from the Canu pipeline (N50 of 9.0 kbp) and the Illumina paired-end reads were used by MaSuRCA [73] to generate a hybrid assembly, resulting in an assembly of 108.1 Mbp, with scaffold N50 of 264.9 kbp and longest scaffold in 2.7 Mbp. A graph-based scaffolder MeDuSa [74] was used to scaffold the Canu contigs based on the MaSuRCA assembly, followed by SSPACE [86] scaffolding using all the mate-pair libraries. The super-scaffolds were first polished by PacBio reads using Arrow v2.2.1 (from SMRT Link v5.0.1) after mapping all the long reads by palign v0.3.1 (from SMRT Link v5.0.1). The PacBio-polished scaffolds were further improved using the paired-end Illumina reads with Pilon [80]. To eliminate putative bacterial contamination super-scaffolds were searched against the NCBI nucleotide (nt) database using MegaBLAST with an (E-value < 1e-65).

De novo repeat finding and repeat masking

A *de novo* repeat identification was performed with RepeatModeler (1.0.8) [83]. Unknown elements were screened with BlastX (E-value < 1e-5) against UniRef91 database [92] (subset Viridiplantae) and removed from the repeat library if necessary. The filtered *Ulva* repeat library was used by RepeatMasker (4.0.7) [82] to mask the repetitive elements in the assembly, which resulted in 34.7 Mbp (35.28%) of the genome masked.

Gene prediction

We applied EvidenceModeler [65] to predict gene models. The consensus gene models were reconciled using the models from *ab initio* and orthology-aided predictions, transcripts reconstructed from RNA-Seq, and homologous models derived from the protein alignments of the available public resource (Figures 5B and S5A). We used BRAKER1 v1.9 [60] to predict the gene models incorporating the RNA-Seq mapping results generated using HISAT2 v2.0.5 [68]. We further used Augustus v3.2.3 with the trained data from BRAKER1 and the protein profile extension to re-predict the gene models [59]. Protein profiles were generated by processing the missing family identified after gene family assignment using OrthoFinder v2.1.2 [76] with the following reference sequence from Phytosome v12.1: *Chlamydomonas reinhardtii* v5.5, *Coccomyxa subellipsoidea* C-169 v2.0, *Dunaliella salina* v1.0, *Gonium pectorale* (assembly ASM158458v1) and *Volvox carteri* v2.1. In addition to the *ab initio* prediction, the RNA-Seq data were also used to reconstruct the transcripts, which consisted of consensus transcripts predicted by Scallop v0.10.2 [84] and predicted coding regions of Trinity v2.4.0 [88] assemblies (both *de novo* and genome-guided) using PASA [65]. Spliced alignments of proteins from UniRef91 (with taxonomy ID 33090) and the FrameDP-corrected [67] and predicted proteins sequence of green algal transcriptomes in the oneKP project [93] were generated using Exonerate [66] seeded by Diamond [64]. We combined the aforementioned gene models with the alignments of proteins, annotation of repetitive elements to produce a consensus gene set using EvidenceModeler. Non-coding RNA and tRNA were identified using Infernal v1.1 [70] and tRNAscan-SE v1.31 [89], respectively. Gene models were functionally annotated using InterProScan 5.27-66 [71] and uploaded to the ORCAE platform [56], enabling members of the consortium to curate and manually annotate. Transcription factors (TF) and transcriptional regulators (TR) were annotated by first screening the proteins for domains and then applying a domain-based rule set [23, 94].

Genome completeness

Completeness of the predicted *Ulva* gene space was evaluated using BUSCO [61] and the coreGF analysis [63]. Core gene families were defined as gene families shared among all *Chlorophyta* present in pico-PLAZA v. 2.0 [79]. In total 1,815 gene families were compared by sequence similarity to the *Ulva* gene models and the reference protein sequences. We assigned each *Ulva* gene model to a particular gene family based on the top 5 hits (E-value < 1e-5). Finally, a GF score was calculated as the sum of each core family identified, counted with a weight equal to one divided by the average family size. Hence, a GF score of 1 indicates that all the core gene families were identified, while a GF score of 0 indicates that no core gene families were found. The likelihood of the presence of each core gene family was calculated for *Ulva* gene models.

Comparative genomic analyses

For the comparative genomic analyses a custom version of Pico-Plaza [79] was built containing genomes and annotations of 32 eukaryotic species (Table S7). Following an 'all-versus-all' blastP [95] protein sequence similarity search, both TribeMCL v10-201 [87] and OrthoMCL v2.0 [77] were used to delineate gene families and subfamilies. Collinear regions (regions with conserved gene content and order) were detected using i-ADHoRe 3.0 [69] with the following settings: gf_type = TribeMCL gene families, alignment method = gg2, number of anchor point s=5, gap size = 30, cluster gap = 35, tandem gap = 30, q-value = 0.85, probability cut-off = 0.01, multiple hypothesis correction = FDR and level_2_only = false. The phylogenetic profile of TribeMCL gene families (excluding orphans) retrieved from pico-PLAZA and the inferred species tree topology were provided to reconstruct the most parsimonious gain and loss scenario for every gene family using the Dollop program from PHYLIP v3.69 [78]. Gene family losses and gains were further analysed by examining the associated Gene Ontology (GO) terms and InterPro domains. Functional information was retrieved using InterProScan [71].

From TribeMCL gene families, highly conserved families were defined as single copy gene families present in all 20 species (*U. mutabilis*, 3 Chlorophyceae, 6 Trebouxiophyceae, 6 prasinophytes and 4 Streptophyta). A concatenated alignment of 58 single copy genes (42,401 amino acid positions) was used to construct a phylogenetic tree using RAXML v8.2.8 [81] (model PROTGAMMAWAG, 100 bootstraps).

Horizontal gene transfer

To search for HGTs, a blast search *U. mutabilis* proteome (blastp, E-value < 10⁻⁵) was carried out against a reduced RefSeq database complemented with data from several algal genomes [96]. The top 1,000 Blastp hits (sorted by bit score) from each query were parsed via custom scripts to extract ≤ 12 representatives from each phylum to create a taxonomically diverse sample. The blastp hits were re-ordered according to query-hit identity followed by the sampling of another set of representative sequences. The query sequence was then combined with the sets of sampled representative sequences following Qiu et al. [96]. A custom script was used to sort trees consisting of *U. mutabilis* that was nested among prokaryotes with at least 80% bootstrap supports. Candidate HGT sequences were then reanalyzed using IQtree v1.4.3 [72] with the built-in model selection function, and branch support estimated using ultrafast bootstrap (UFboot) with 1,500 bootstrap replicates (-bb 1,500). Last, we visually confirmed that the putative HGT genes were an integral part of long sequencing reads and flanked up and downstream by non-HGT genes.

Phytohormone bioassay and measurements

Endogenous phytohormones were extracted from thalli (3-weeks-old) and axenic cultures (12.5 mg·mL⁻¹) by the acidified polar solvent 80% acetonitrile and 1% acetic acid in water (v:v) upon maceration through a tissue lyser (Qiagen, Germany). Compounds were purified to eliminate interferences by multiple steps of solid-phase extractions [97], and quantified by UHPLC-ESI-MS/MS (LC system equipped with a C18- Kinetex column (dimensions: 50 × 1.7 mm, Phenomenex, USA) and coupled to a Q Exactive Quadrupole-Orbitrap mass spectrometer (Thermo Fisher Scientific, UK). Deuterium-labelled standards (d₅-IAA, d₆-ABA, d₄-SA; ChemIm Czech Republic) were used for quantification. The limit of detection was in the range of 0.8 - 8.0 fmol on the column, whereas the limit of quantification was in the range of 2 - 20 fmol on column depending on the phytohormone. Ethylene emanation was measured by laser photo-acoustics [98].

To test if morphogenesis of *Ulva* into a blade- or tube-like thallus may require specific phytohormones, gametes were inoculated with ABA, GA₃, IAA, JA, SA and ZEA at a final concentration of 10⁻⁶ and 10⁻⁹ mol/l. Control treatments consisted of inoculating *Ulva* gametes with bacteria (final optical density 1×10⁻⁴). Development was monitored for 2 weeks.

Measurement of DMSP and qPCR

Expression of DMSP lyases (UM030_0039, UM021_0036), putative S-adenosyl-L-methionine-dependent methyltransferases (UM052_056, UM036_0102) and BCCT transporters (UM033_146, UM033_147, UM033_150, UM033_150) was examined in xenic and axenic 4-5 week-old thalli grown at 8°C or 18°C using qPCR (Table S8). Expression values are based on at least 4 biological replicates. DMSP was measured in xenic thalli grown under both temperatures as outlined in Kessler et al. [47] (n = 12). RNA was extracted from *Ulva mutabilis* (slender strain) using the Spectrum Plant Total RNA Kit (Sigma), including the optional DNaseI digestion, and 500 ng was reverse-transcribed with the PrimeScript RT-PCR Kit (Clontech). qPCR reactions were performed using SYBR Green Master Mix (Clontech) on a BioRad CFX96 Real-Time PCR Detection System. Primers are listed. Transcript abundance was determined according to the Pfaffl method [99]. For normalization of expression levels, we used the reference genes UM008_0183 (Ubiquitin) and UM010_0003 (PP2A 65 kDa regulatory subunit A).

QUANTIFICATION AND STATISTICAL ANALYSIS

Enrichment and depletion of InterPro domains in *Ulva* and *Caulerpa* were tested using a Fisher's exact tests with a false discovery rate correction (Benjamini-Hochberg FDR method) of 0.05. Interpro domains, proven to be significantly depleted or expanded were grouped at Superfamily-level to reduce redundancy. Fisher's post hoc tests were used to determine significance of expression values of DMSP lyases (n = 4 or 8), methyltransferases (n = 4) and BCCT transporters (n = 4). All statistical tests were carried out in R [100]. Phylogenetic trees were reconstructed using either RAxML v8.2.8 [81], IQTree v1.4.3 [72].

DATA AND SOFTWARE AVAILABILITY

The assembled genome sequence, annotation and raw reads are accessible from ENA under BioProject number PRJEB25750. Further information on the *Ulva mutabilis* project is available via the Online Resource for Community Annotation of Eukaryotes (ORCAE) at <http://bioinformatics.psb.ugent.be/orcae/>.